Journal of Structural Geology. Vol. 1, No. 1, pp. 31 to 42.
Pergamon Press Ltd. 1979. Printed in Great Britain.

Orthogneiss, mylonite and non coaxial deformation of granites: the example of the South Armorican Shear Zone

D. BERTHÉ, P. CHOUKROUNE and P. JEGOUZO

Centre Armoricain d'Etude Structurale des Socles, C.N.R.S., Université de Rennes I, Avenue du Général-Leclerc, 35042 — Rennes—Cédex, France

(*Received* 14 *September* 1978; *accepted in revised form* 19 *December* 1978)

Abstract—The deformation of two granitic massifs along a dextral wrench fault zone (the South Armorican Shear Zone) is examined at the sample and grain scales. We note that an association of continuous–discontinuous deformation mechanisms is responsible for the mylonitisation at the grain scale. The general characteristics of the deformation (strain, ellipsoid type, strain regime, non-coaxial model) and quartz fabrics measured in these mylonites at each of the mylonitisation stages described, are also discussed.

Résumé—La déformation de deux massifs granitiques impliqués dans une zone de décrochement dextre (le cisaillement sud-armoricain) est essentiellement étudiée à l'échelle de l'échantillon et du grain. A de telles échelles, on met notamment en évidence l'association de déformations continues et discontinues responsables de la mylonitisation de ces granites. Les caractéristiques générales de la déformation (type de l'ellipsoide de déformation, régimes, modèle de noncoaxialité) et la fabrique du quartz relevée dans ces mylonites à divers stades de l'évolution de la mylonitisation sont par ailleurs discutées.

INTRODUCTION

Definition of the problem

THE AIM of this contribution is to examine the different stages of the development of orthogneiss (orthogneissification) from granites which have undergone progressive deformation in a major crustal shear zone in the Hercynian chain. Deduction is largely based upon deformation at the grain scale, under known conditions (deformation approximating to simple shear with a dextral relative movement sense), and where the starting material is granular and isotropic (observed outside the shear zone).

This deformation may be described: (i) *from a descriptive point of view,* the evolution of the deformation is followed from the initial through to the terminal, most deformed state, and the different stages of orthogneiss development as well as the first appearance and evolution of the associated microstructures are considered; (ii) *in relation to the deformation mechanisms,* paying particular attention to the continuous and discontinuous processes responsible for the deformation of the grains at each of the stages described; (iii) *in relation to strain regimes* (flattening and shearing) deduced from the observation and interpretation of the microstructures.

Structural setting of the example studied

It is known that the late-Hercynian was a time of lithospheric fracturing (Arthaud & Matte 1975) (Fig. 1a) which resulted in the creation, throughout Western Europe, of a coherent network of dextral and sinistral wrench faults of variable size and magnitude, the significance of which must be considered on the scale of a continental plate (Arthaud & Matte 1977).

The dextral South Armorican Shear Zone is one of these major fracture zones extending for more than 400 km from west to east (Fig. 1b) between the western extremity of Brittany to the Vendée–Poitou region. Although all the rocks which it cuts have undergone Hercynian orogenesis, the shear zone brings into contact blocks which differ greatly from one another from the point of view of structural evolution (Cogné 1960, 1966, 1977).

Within the, undoubtedly already initiated fracture zone and in immediately adjacent areas, biotite–muscovite granites, dated at approximately 320 Ma (Vidal 1973), were emplaced. The deformation of these granites, by dextral shearing, along the South Armorican Shear Zone forms the subject of this work. It must be emphasized that this example of non coaxial deformation, at all scales, concerns an isotropic starting material, which has not been disturbed by deformational events other than the single major event discussed here.

The material studied

This study was carried out on two leucogranite bodies situated along the two distinct branches of the South Armorican Shear Zone (Figs. 2a & b). The first of these bodies, located on the northern branch, comprises a medium grained (2–5 mm) isotropic granite. The second, on the southern branch, consists of an equally isotropic but finer grained granite. The mineralogical compositions of the two granites are very similar, each rock type comprising; quartz, K-feldspar, plagioclase (An 10–15), biotite, muscovite, plus accessory minerals. The zone of deformation affecting the granites is between 1.5 and 2 km in width. Within the northern granite the deformation increases from north to south. The deformation in the southern granite diminishes on either side of a central more intensely deformed belt (symmetric zone) (Fig. 3). These strain gradients are expressed in the field by a succession of classical cataclastic deformation stages; protomylonites, mylonites,

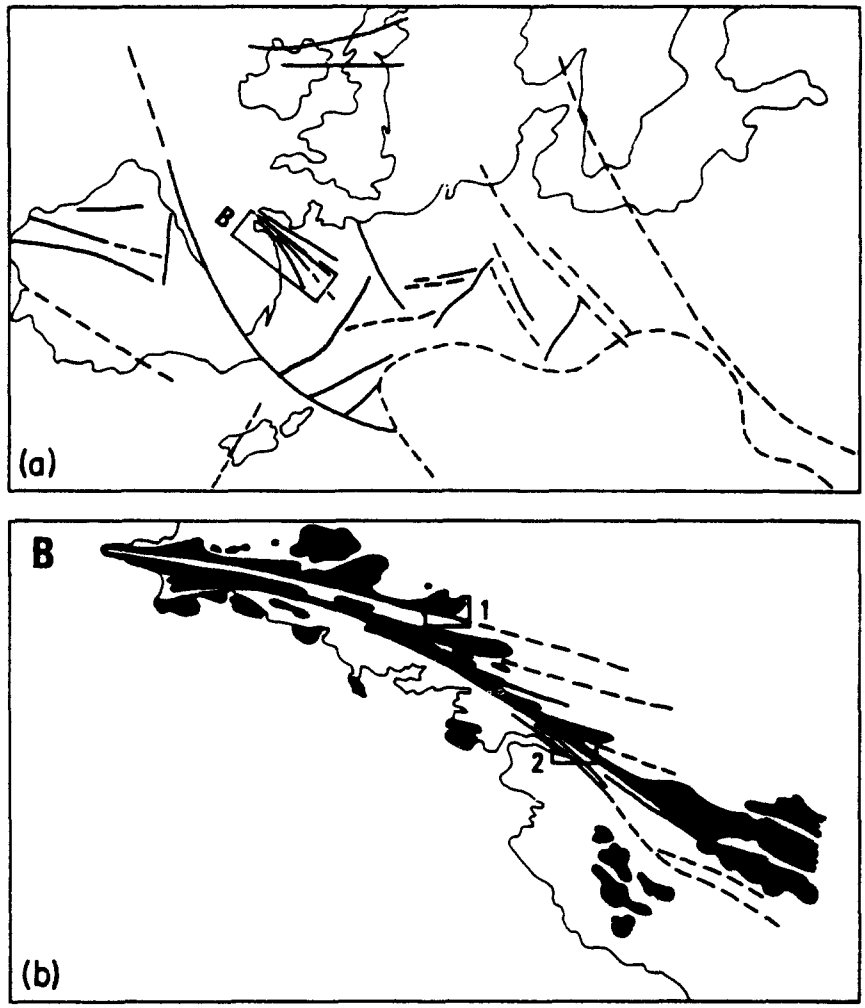

Fig. 1. (a) The South Armorican Shear Zone in the context of late-Hercynian wrench faulting (after Arthaud & Matte 1977). (b) Location of Hercynian leucogranites and massifs studies: (1) northern massif (2) southern massif.

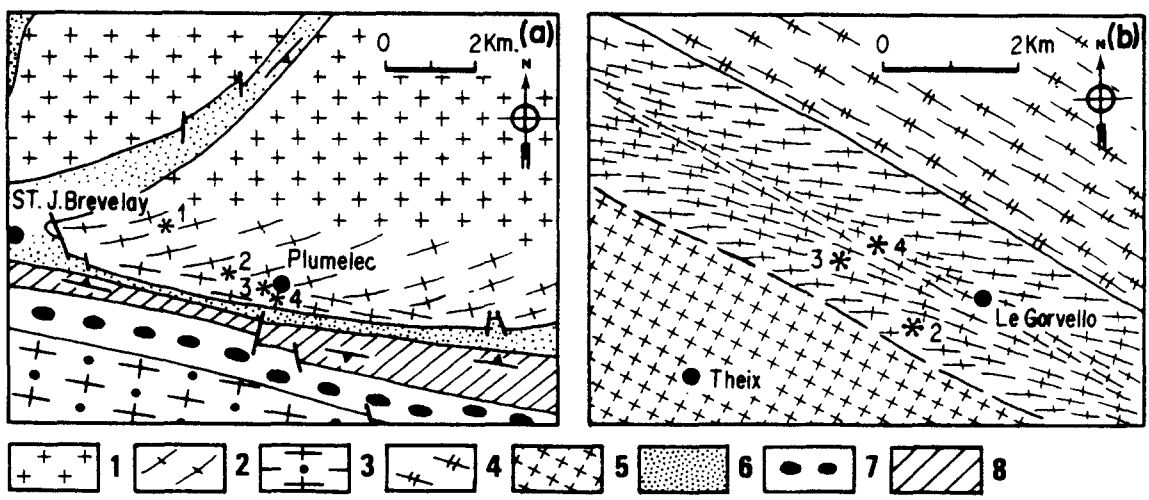

Fig. 2. Schematic geological map of the studied areas. (a) northern massif. (b) southern massif. *Ornament:* 1 — Isotropic two mica granites, 2—mylonitic gneisses, 3—orthogneiss de Lanvaux, 4—isotropic two mica granites (coarse grain), diatexite and migmatites, 6—Brioverien, 7—schistes et arkoses de Bains-sur-Oust, 8—Lower Palaeozoic. Small numbers on maps refer to sample localities.

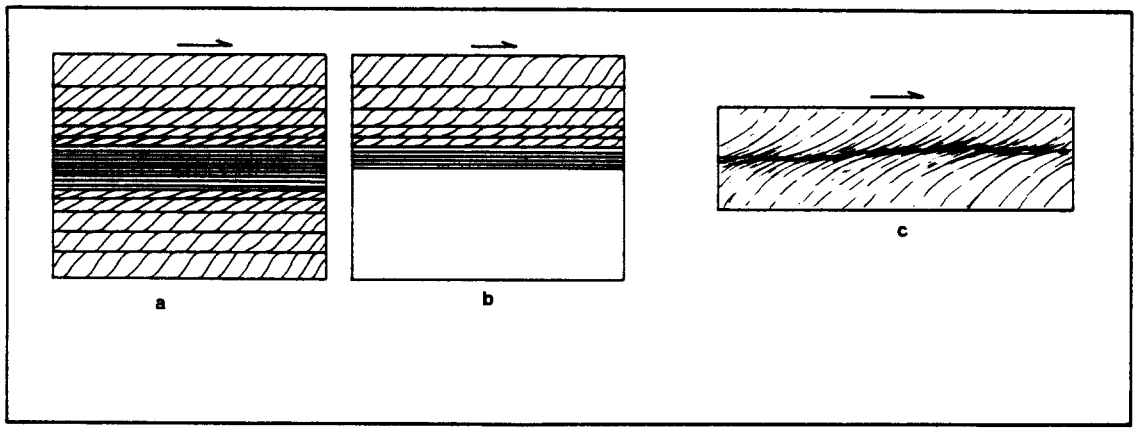

Fig. 3. Diagrammatic representation of the shear zones. (a) in the southern granite, (b) in the northern granite and (c) model of ductile shear zone adapted from Ramsay & Graham (1970).

and ultramylonites (Higgins 1971). Within the central zone of the southern granite, the most advanced stages of orthogneiss development are seen; however, hyalomylonitic textures have not been observed.

THE EVOLUTION OF THE DEFORMATION

First appearance and evolution of planar and linear anisotropies

The most remarkable feature is the appearance, at a little deformed stage, of two sets of surfaces of which one maintains a constant orientation within each deformed band. Such a set of surfaces, subvertical and striking 100–110° in the northern granite and 120–125° in the southern granite where they bear a subhorizontal lineation, is parallel to the cartographic trace of the major shears. The lineation clearly corresponds to the projection on the surfaces of a stretching direction related to deformed minerals. On these same surfaces and parallel to this lineation, are slickenside striations present at all stages of the deformation. These surfaces are therefore planes of relative movement along which there was an essentially horizontal sense of displacement (C surfaces on Fig. 4).

The second set of surfaces, also subvertical, but oblique to the first set, define the plane of preferred mineral orientation (Fig. 4). During the initial stages of orthogneiss development the angle between the two sets of surfaces is approximately 45°. Phyllosilicate mineral cleavages (001) tend to be parallel to the orientation of this second set of surfaces, which contains the maximum extension direction of the deformed minerals. This planar anisotropy therefore corresponds to a schistosity (S surfaces), i.e. the XY plane of the finite strain ellipsoid during the initial stages of the deformation. This inference is supported by the observation that pressure-shadows at the extremities of feldspar porphyroclasts, are contained in the S surfaces.

When orthogneiss development intensifies, the angle between the two sets of surfaces, close to 45° in initial stages, diminishes progressively by rotation of the S surfaces, whereas the C surfaces maintain an approximately constant orientation. As the ultramylonitic stage is approached, this process results in a degree of parallelism between S and C surfaces such that they can no longer be distinguished (CS surfaces).

Within this progressive evolution, we have distinguished four stages (Fig. 5). At the initial stage, the angle (α) between the C and S surfaces is equal to 45°; at the

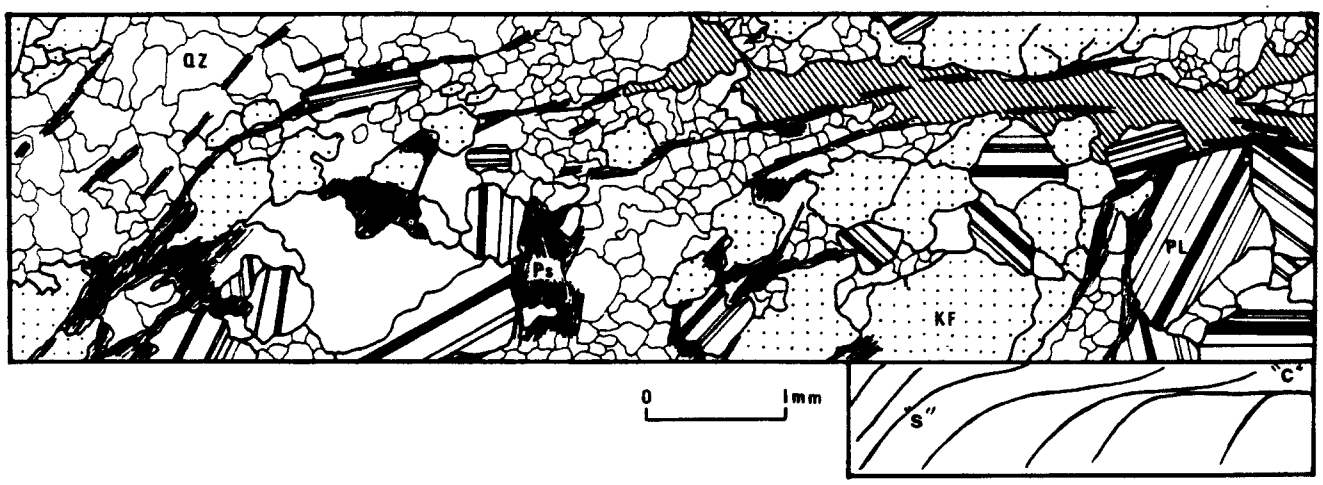

Fig. 6. The deformation at the extremity of a C surface and the problem of attenuation of discontinuous movement by ductile deformation. The S surfaces adopt a sigmoid configuration before anastomosing with the C surfaces. In the shaded part, the comminution is well advanced. Qz—quartz, Ps—phyllosilicates, KF—potash feldspar, Pl—plagioclase.

second stage, the average value of α is 25°; at the third, this value is 10° and the fourth stage, the two sets of surfaces are subparallel.

Accompanying the decrease in the value of α, the density of C surfaces increases. Density values (number of C surfaces per centimetre thickness of rock) increase from 1 to 10 between stages 1 and 3. Density values for C and S surfaces at stage 4 are very high indeed.

It is necessary to comment on three aspects of the preceding observations. At the initial stage, the rock is affected by two types of vertical surfaces, orientated at 45° to each other; planes of shearing (C planes), and passive planes (S planes). At this stage, the C surfaces are weakly developed, parallel to the shear direction and range from several centimetres to several tens of centimetres in length. The extremities of these surfaces correspond to zones of attenuation of slip along the C discontinuities. Such attention appears to occur by continuous deformation at the grain scale and is indicated by the tendancy of S surfaces, in such zones, to adopt a sigmoidal shape as they trend towards parallelism with the shear direction (Fig. 6). The increase in the density of C surfaces results from two distinct but related processes: (a) the creation of new dextral shear planes; and (b) the activation of S surfaces, which become more and more evident as the angle α diminishes. In effect, the S surfaces becomes dextral relative movement surfaces when α is close to 15°. At the most advanced stage, asymmetric folds develop which deform the unique plane anisotropy, and whose configuration is compatible with the dextral shear sense (Fig. 7).

The evolution of S and C planes can be interpreted schematically if one examines the deformed bands in their totality (Fig. 3). In the southern granite, at the mapping scale, the configuration of the S surfaces conforms to that described by Ramsay & Graham (1970) in ductile shear zones. In the northern granite, only a half-shear zone is visible. In both granites, the C surfaces, with their nearly constant orientation, form a set of microstructures which should be added to the ductile shear model.

Initial appearance and development of mylonitic deformation

It is well-known that in mylonite zones, an increase in the intensity of deformation is expressed by a decrease in grain size, accompanied by recrystallization. This

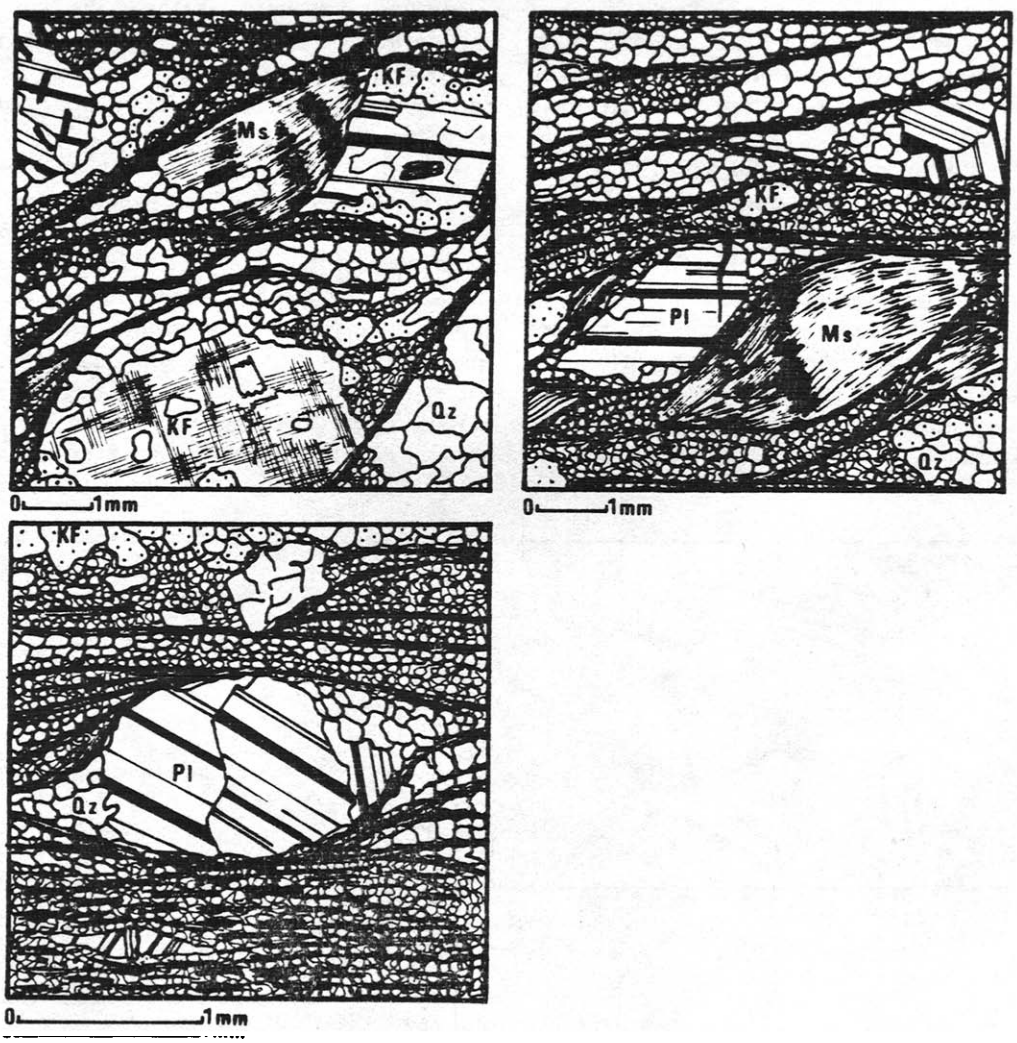

Fig. 8. Three stages in the evolution of the mylonitization: cataclastic processes tend to produce a reduction in grain-size and increase in the number of cataclastic C surfaces. The ultramylonitic stage of the central zone from the southern granite is not figured. Qz—quartz, Ms—muscovite, KF—potash feldspar, Pl—plagioclase.

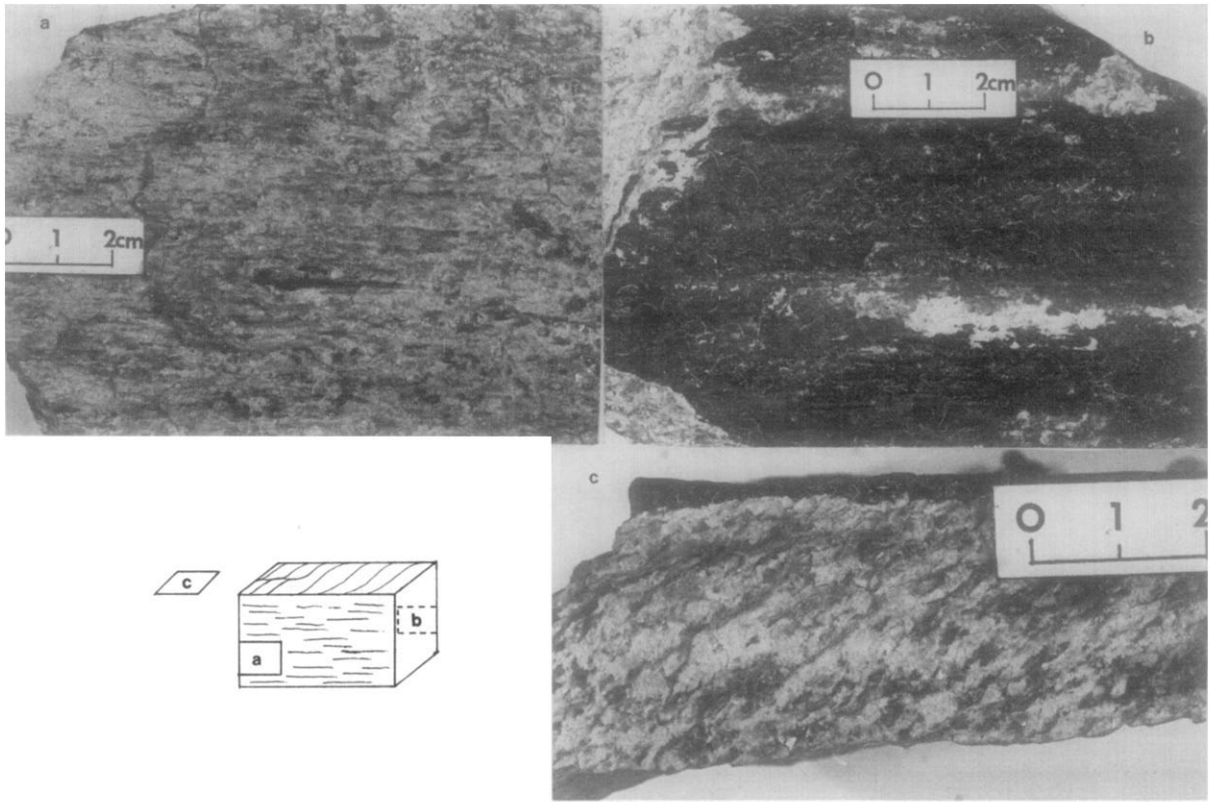

Fig. 4. On the C surfaces, (a) and (b), the lineation is parallel to slickensides. The relationship between C and S surfaces is illustrated in (c). See text for details.

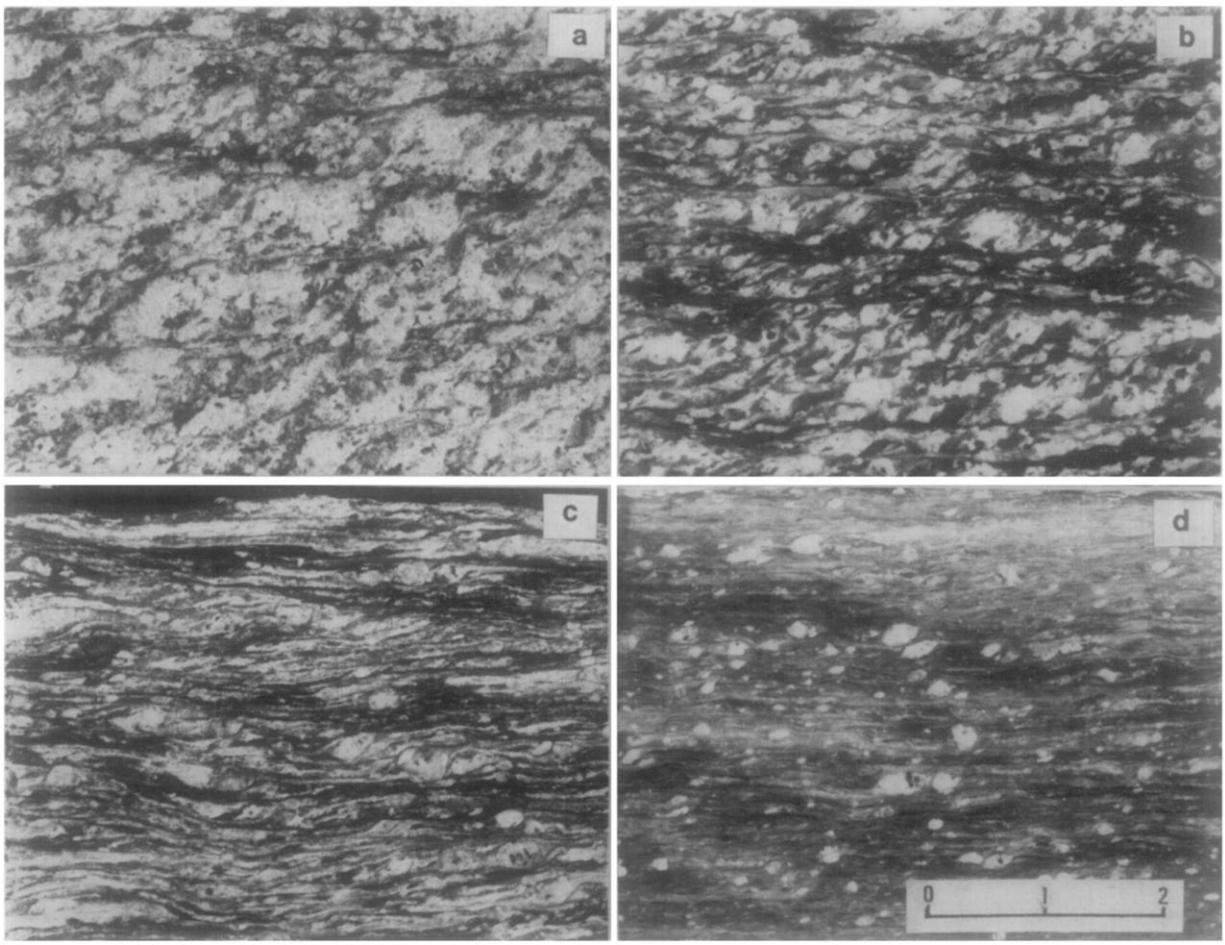

Fig.5 The four stages distinguished in the evolution of the angle (α) between C and S surfaces. (a) $\alpha = 45°$, (b) $\alpha = 25°$, (c) $\alpha = 10–15°$, (d) $\alpha = 0$. Scale bar for all photographs is 2 cm.

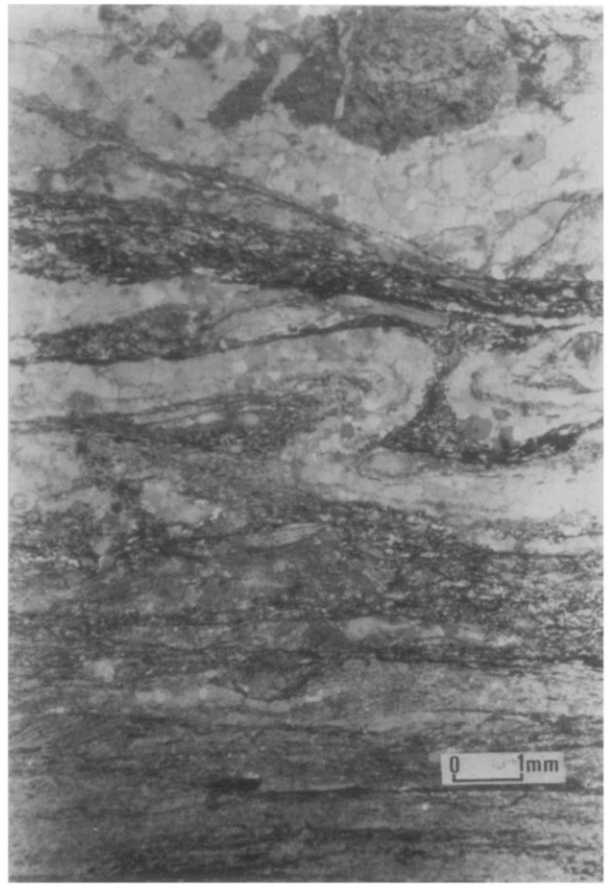

Fig. 7. Asymmetric microfold deforming the S and C surfaces compatible with the proposed dextral simple shear. Scale bar is 1 mm.

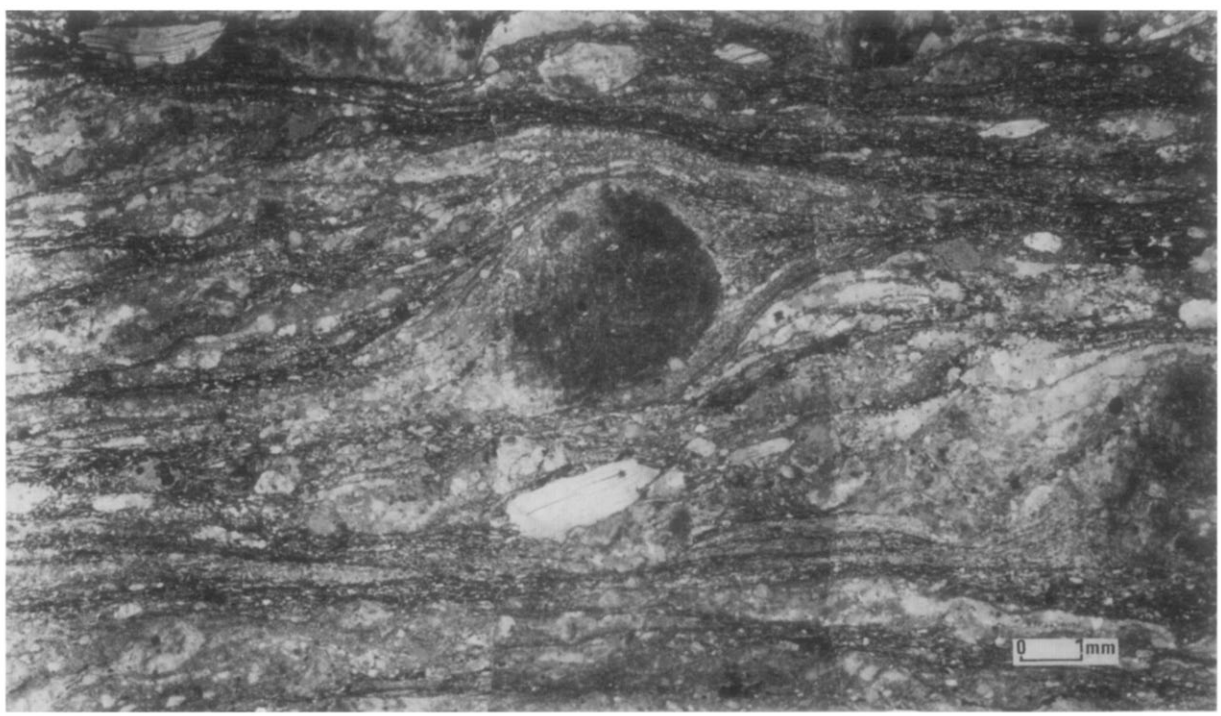

Fig. 10. The obliquity of X (incremental) during the last increments of deformation shows that, at this stage of the deformation, the S surfaces no longer constitute the XY plane of the finite strain ellipsoid. Scale bar is 1 mm.

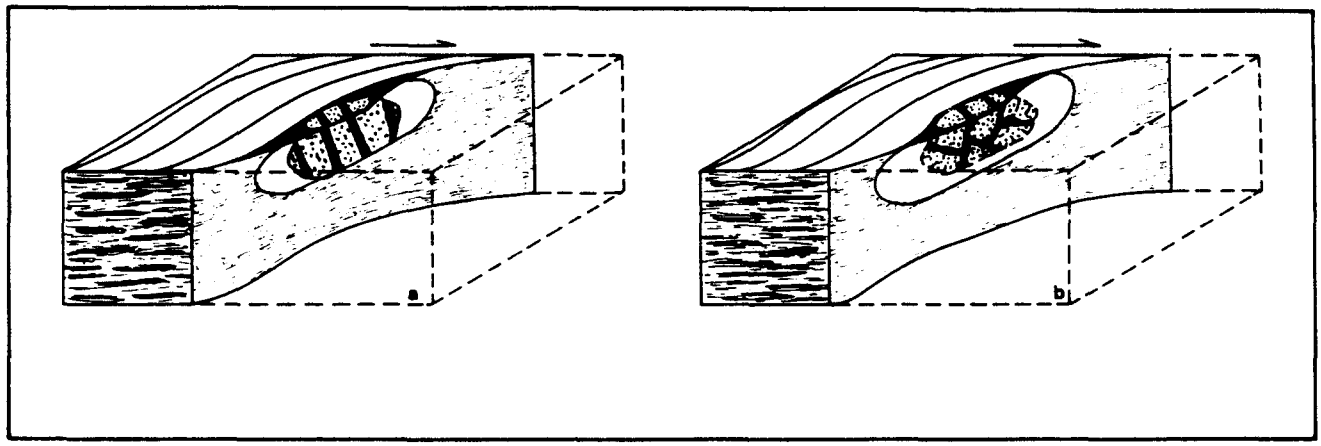

Fig. 9. Use of the deformation of feldspathic clasts and pressure-shadows for the determination of the sype of strain ellipsoid. (a) plane strain or constriction, (b) flattening.

progressive decrease of average grain size is here seen to accompany a decrease in angle between C and S surfaces. In the northern granite, mylonitization increases from north to south and is accompanied by recrystallization of quartz, fine grained albite, biotite and microcline. The cataclastic fraction (we define the cataclastic fraction as that fraction of the rock composed of deformed minerals, irrespective of the process of deformation) is everywhere more important than the recrystallized fraction. Thus, one passes from a protomylonitic stage through to a ultramylonitic stage in which only a small proportion of feldspar phenoclasts remains in the fine grained (average grain size 10 μ) matrix.

The process, illustrated by three stages in Fig. 8, may be summarised as follows. As mylonite development progresses, the size of orthoclase and plagioclase phenoclasts diminishes at the same time as comminution at their margins increases. The secondary crystallisation of quartz and fine microcline within protected zones, or pressure-shadows, located at the extremities of phenoclasts also becomes increasingly important.

The ends of phyllosilicate grains (biotite, muscovite) are comminuted at their contacts with C surfaces, whilst their (001) cleavages, initially parallel to S surfaces, show a clear tendency to slip. An elliptical outline and undulate extinction in the phyllosilicates is produced relatively early in the deformation.

Quartz recrystallizes from the protomylonitic stage onwards, forming large elongate polycrystalline grains parallel to S surfaces. These grains later tend towards parallelism with C surfaces.

At all stages in the process of mylonite development, in the immediate neighbourhood of C surfaces, a residue of quartz, feldspar and mica, as well as recrystallized quartz, is present and displays a finer grain size than average for the rock.

In the southern granite, the same sequence as just described can be followed from the margins towards the centre of the deformed zone, the distribution of deformation features being fairly symmetrically disposed about the centre line.

In the initial stages, C surfaces are principally lined with quartz and micas (biotite, muscovite) of approximately 10–30 μ grain size. An internal crystallographic fabric may sometimes be observed in the quartz. Between C surfaces, the grain size is generally close to that of the original granite, with the exception of quartz which recrystallizes as coarse new-grains (150–300 μ) with lobate or frilled margins, aligned parallel to the S surfaces. The basal (001) planes of the micas are equally aligned in the S surface orientation, whilst in outline they may be lozenge shaped where truncated at their contacts with C surfaces. The feldspars, however, generally fracture along their cleavages, the opened cracks being welded with a quartz fill (Fig. 9).

The increasing number of C surfaces leads progressively to the incorporation within such surfaces of the constitutive minerals of the rock (quartz, micas, feldspars). At the ultramylonitic stage only a few clasts of K-feldspar (with pressure-shadows oblique to the C and S surfaces) remain in a very fine grained, layered matrix. This fine layering, with individual layers rarely exceeding 1 mm in thickness, is related to an alternation of layers rich in quartz and mica, with those rich in feldspar debris.

The microscopic characteristics of the cataclasis in the two cases studied are closely comparable. This is true for the relatively similar behaviour of different minerals during the cataclastic process, as well as for the thermodynamic stability, or instability, that the observed assemblages allow one to estimate. In both cases, muscovite, fresh brown biotite, albite and microcline are stable and may even have recrystallized.

Finite strain and mylonitization

The only qualitative strain marker in the mylonites is the presence at the ends of feldspar phenoclasts of pressure-shadows whose long axes are assumed to give the average orientation of the X axis of the last incremental strain ellipsoid. This direction lies entirely within S surfaces in the initial, little deformed stages, and makes an angle of 45° with C surfaces. X remains oblique (with a small angle of 10°) to C and S surfaces in the most advanced stages of the deformation. It follows therefore that, during deformation, S surfaces rotate

more rapidly than the X axis. This deformation is therefore a typical non coaxial deformation in the XZ plane (Choudroune & Lagarde 1977) (Fig. 10).

The form of the strain ellipsoid during the last increments of deformation is given by the form of the pressure-shadows contained in the S surfaces. They show in some cases that there was local extension along the Y axis (flattening), at least during these last increments. In other examples, shortening along Y axis is indicated by the presence of either or both pressure solution and comminution normal to this axis (Fig. 9). We interpret these slight variations as fluctuations about an average value of K close to 1 (plane strain).

Petrofabric data

In the northern sector, quartz petrofabric data were obtained with an universal stage for different stages of the deformation as estimated from the angle α between S and C surfaces (Fig. 11). In the specimens from the southern sector, quartz was analysed using a texture goniometer. A statistical spatial representation of normals to $(10\bar{1}0)$ (axis m) prismatic faces, and $(10\bar{1}4)$ (angle with C axis = 17°) was plotted (Fig. 12).

In both sectors, from the initial stages of the deformation onwards, a clear quartz fabric is present. In both cases, the fabric is of girdle type, and contains a marked concentration of C axes parallel to the Y axis of the finite strain ellipsoid. This is compatible with plastic deformation by dominantly prismatic slide (Bhattacharya & Pasayat 1968, Laurent & Burg 1978). The southern sector is distinguished by a disorganization of the fabric which starts to become evident in the intermediate stages of the deformation, and results in a near total destruction of the fabric in the ultramylonitic stage. Such fabric destruction might be explained for the most developed stages by a change of deformation mechanism, very probably related to the decrease in the size of the grain size (Schmidt *et al.* 1977, White 1976), and by the initiation of a dominantly grain boundary slip deformation mechanism (Boullier & Guegen 1975).

INTERPRETATION

Non coaxial deformation model

The sense of shearing, deduced from microstructural and field observations, is dextral and thus compatible with data collected during mapping. It should be noted that the oblique character of quartz C fabric girdles in the YZ plane constitutes an additional argument in favour of a deformation in which the X and Z axes rotate in a dextral sense about the Y axis at each increment of strain. The model of deformation in the two granitic bodies can therefore be represented by the development of a dextral simple shear increasing in

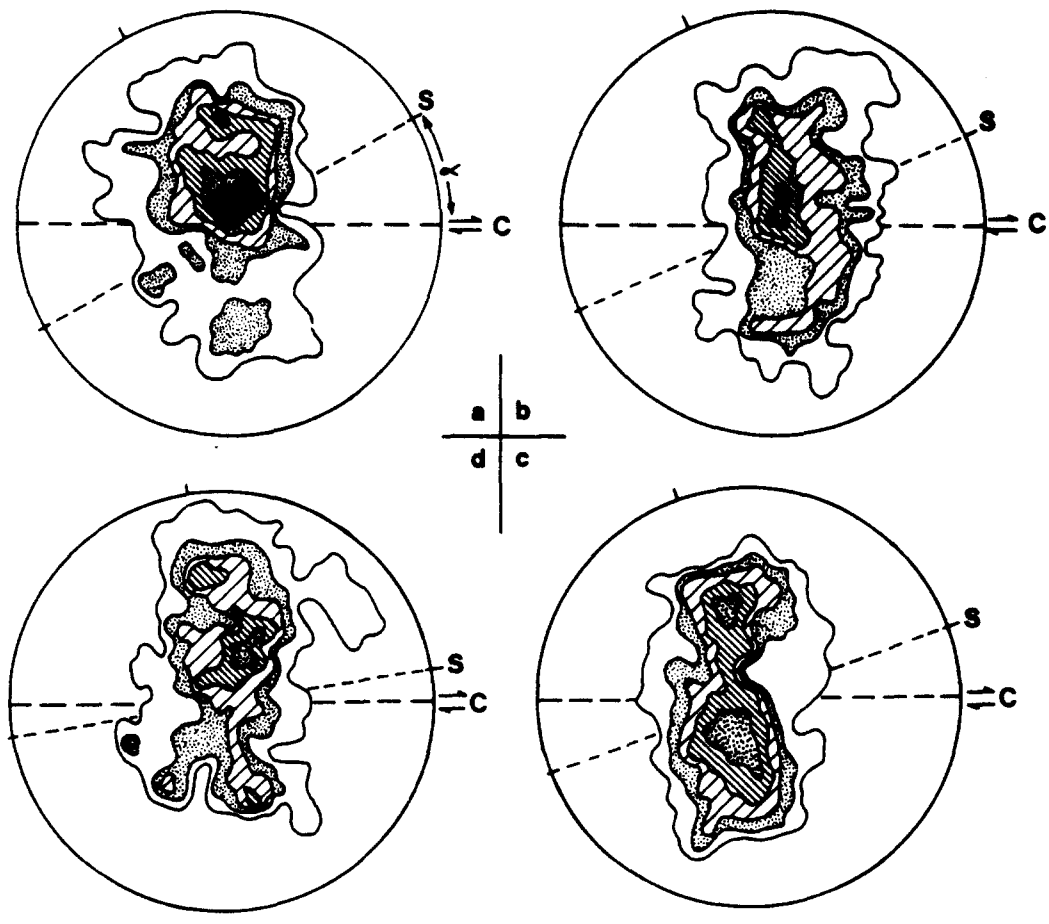

Fig. 11. Quartz C-axis petrofabric diagram (lower hemisphere) for the northern sector. (a) 320 points α = 30°, (b) 350 points α = 25°, (c) 320 points α = 20°, (d) 310 points α = 10°. Contours at 1, 2, 3, 4, 5, and 6%.

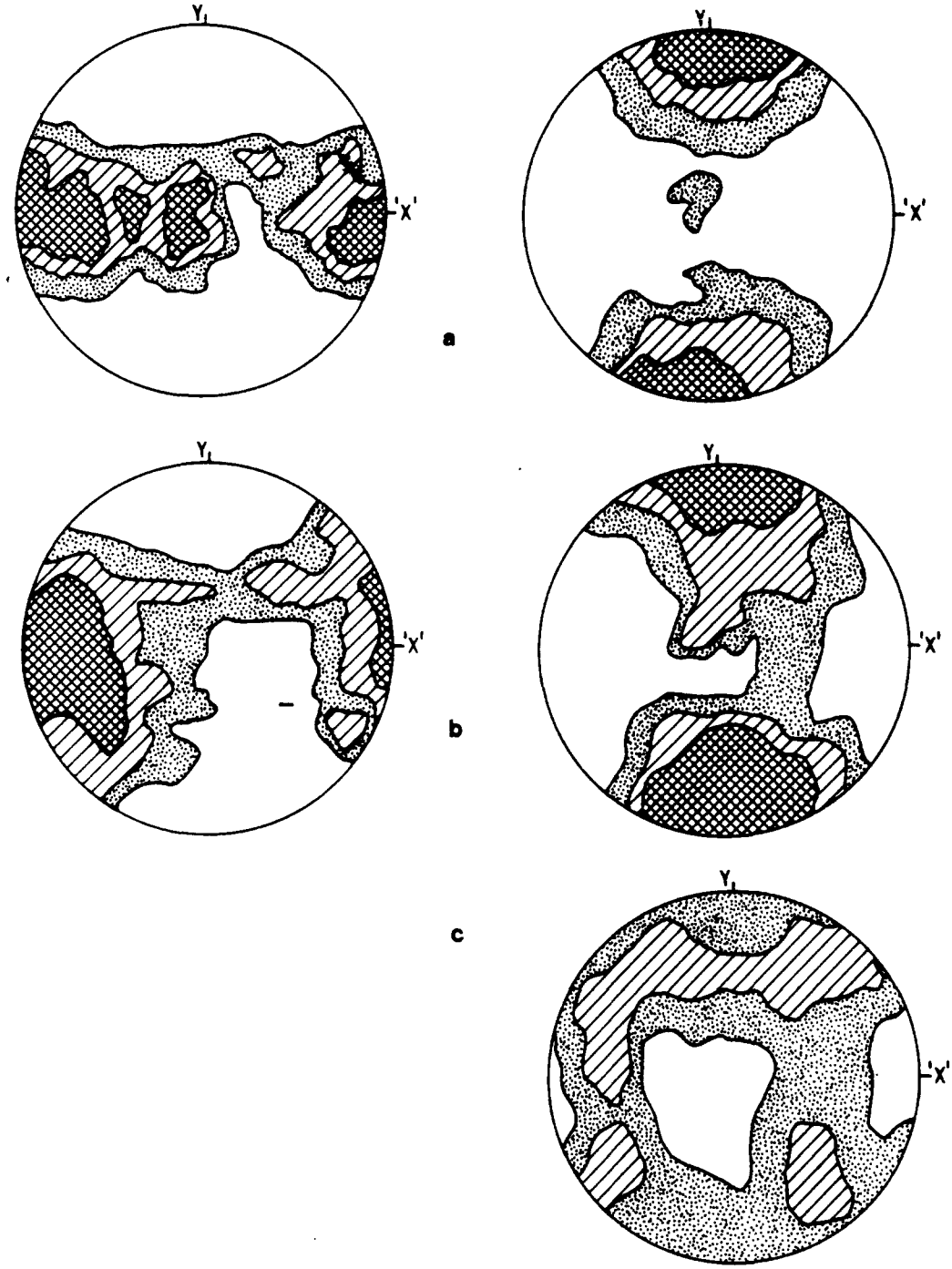

Fig. 12. Preferred orientation of quartz (southern sector). Pole diagrams obtained by texture goniometry and projected on the plane of C surface (lower hemisphere). The contours correspond to multiples of the average density (A.D.). Left column shows *a* axis (1120). Right column shows (1014) axis (angle with C-axis 17.7°). (a) initial stage = 1,1.5, 2 × A.D., (b) intermediate stage = 1,1.2,1.4 × A.D., (c) terminal stage = 1,1.5 × A.D. (the destruction of the the fabric is already evident).

intensity from north to south in the northern granite or towards the centre of the zone in the southern granite.

However, the inference that K values fluctuate about 1.0 indicates that the deformation, although globally involving plane strain for each deformed area, passes locally into flattening or constrictional fields. It must therefore be supposed that, at the scale of a hand specimen, the deformation consists of two components; a simple shear and a limited pure shear. There is no structural evidence to suggest that these two components were separated in time, in contrast to certain recently described shear zone models (Roy 1977).

Finally, the constant presence of C surfaces, in so much as they represent planes of discontinuity at the grain scale, shows that the shear zone model is not a purely ductile one (Ramsay & Graham 1970).

The continuous–discontinuous character of deformation mechanisms at the grain scale

In order to discuss the continuous or discontinuous nature of the deformation, it is essential to consider a given scale; here we consider the scale of the average grain size of the rock. For example, quartz grains

showing undulose extinction are considered to have been deformed in a continuous mode. On the other hand, a broken feldspar, fragments of which have been displaced relative to one another, is considered to have been deformed in a discontinuous mode. In the present example, preferred orientation of quartz and bending of mica cleaveges constitutes the evidence for the operation of the continuous mode. Furthermore, the visible displacement of feldspar and mica fragments along the C planes, and the presence of striations along the same demonstrate, the association of discontinuous and continuous deformation at the scale considered.

The examples studied here are, in our opinion, quite remarkable because the co-existence of both continuous and discontinuous deformation at the grain scale can be demonstrated at all stages of the deformation. For example, at the initial stage, in the zones of C surface attenuation, there is a progressive passage from discontinuous to continuous deformation (Fig. 6). This is confirmed by the observation that the zones of cataclasis pass progressively to those affected by internal plastic deformation, as indicated by undulose extinction.

At a more advanced stage, the domains of ductile deformation (S surface domains) are limited by C surfaces where demonstrable, discontinuous relative movements are localized (Fig. 13), and where the cataclasis is the most intense. We emphasize that the ductile deformation domains are increasingly restricted in extent as the rotating S surfaces attain an orientation favorable to their activation as movement planes.

Thus the deformation becomes increasingly discontinuous up to the most advanced stage at which C and S planes are no longer distinguishable, and during which deformation may once again be considered to be continuous on the scale of a grain. Therefore, C and S surfaces are not principal planes of the finite strain ellipsoid as demonstrated by the non-coincidence of these planes with the X axis (Fig. 10).

Finally, the existence of a striation on C surfaces, at all stages of deformation, confirms the active nature of these planes. Such striations are parallel to the apparent stretching lineation on the C surfaces, and thus indicate the coherence of the association of continuous–discontinuous deformation.

P–T estimates of the deformation

If account is taken solely of the petrographical data, the most striking fact concerning the P–T conditions during deformation is the stability of the micas, notably

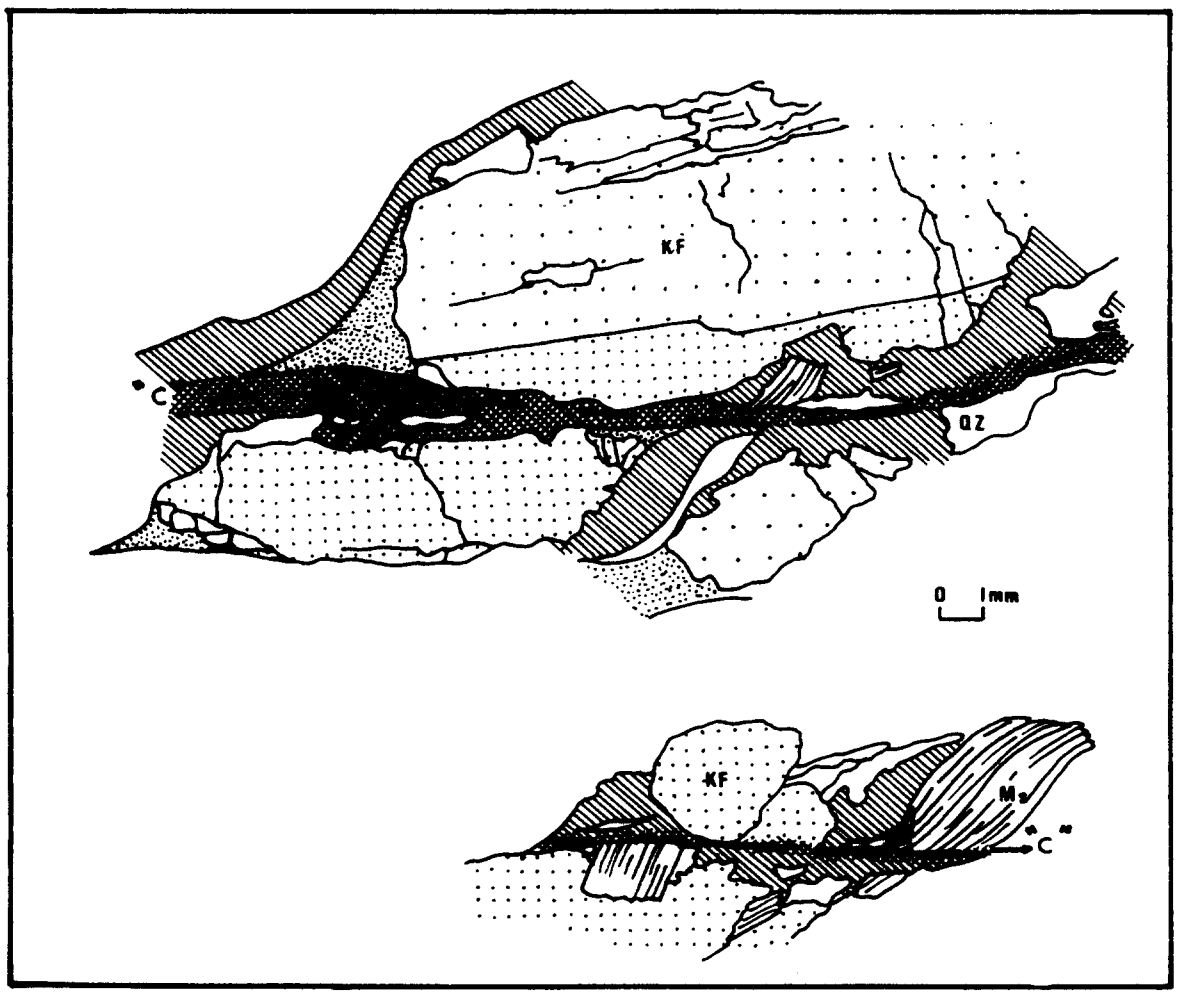

Fig. 13. Discontinuous character of the deformation at the grain scale along C surfaces. In the upper sketch, two fragments of a single K-feldspar grain are offset by 5 mm. The same phenomenon, affecting a muscovite grain, is illustrated in the lower sketch. KF—potash feldspar, Qz—quartz, Ms—muscovite.

that of fresh brown biotite. Chloritization has not been observed in the specimens studied. Recrystallization affects albite and microcline and, to some extent, quartz.

The petrographical data, combined with the tendency to prismatic slip in the quartz, especially apparent in the southern granite, suggests that the deformation took place at relatively elevated temperatures, undoubtedly greater than 400–450°C.

By extrapolating the calculated geothermal gradient associated with the San Andreas Fault (Lachenbruch & Sass 1973) to the South Armorican Shear Zone, for a temperature of 400°C, one obtains values of P (P = confining pressure + fluid pressure) of about 5 kb. Such a value is reasonable, taking account of the general setting of this part of the Hercynian chain. Furthermore, it should be noted that the assemblage albite–microcline is stable at 5 kb and temperatures of less than 500°C (Kroll & Bambauer 1971).

DISCUSSION

The examples studied here provide valuable information on the important question of the association of continuous–discontinuous deformation at the grain scale in the process of mylonite development. We conclude that this association is primary, that is to say, the combination of the two mechanisms occurs at several stages of the deformation up to the stage where grain size is less than the spacing between adjacent anisotropy planes. Such a stage is more advanced however, than that seen in most orthogneisses.

The arguments for the concomitant nature of the deformation mechanisms are as follows. Nowhere are S surfaces present without C surfaces being equally present. Neither are there any examples of C surfaces being developed alone. The development of C surfaces and S surfaces represents a parallel and coherent evolution. The process is evidently related to a progressive variation in the intensity (γ) of shear strain. It is unreasonable to suppose that two successively superposed deformation mechanisms will result in two deformations whose maxima of intensity are spatially coincident. Deformation of the continuous–discontinuous type has been reproduced in model experiments (Means 1977) as well as in deformation experiments performed on granite samples under varied P–T conditions (Tullis & Yund 1977). Such an association of simultaneous deformation mechanisms persists up to elevated temperatures (600°C) (Tullis & Yund 1977). Although, it is evident that the experimental strain rate (in the order of 10^{-6}/s) does not clearly reproduce natural deformation conditions (we envisage a natural strain rate of the order of 10^{-12}/s), we take it as demonstrated that deformation of the continuous–discontinuous type may develop at elevated temperatures.

Finally, the question is posed as to which parameter controls the development of shear zones as described here, or the development of such zones according to the model of purely ductile shear as described at outcrop by Ramsay & Graham (1970), or on mapping scales (Coward 1976, Bossière & Vauchez 1978). In our opinion, the strain rate cannot have been constant and must have varied abruptly during the development of the South Armorican Shear Zone.

CONCLUSION

The process of orthogneiss development as envisaged here is the sum of two distinct deformation mechanisms (continuous–discontinuous) and locally the sum of two deformation regimes (simple shear and flattening) which have, probably, operated at each stage of the process.

One can ask, to what degree: (a) the characteristic features of such a model are typical; and (b) are such characteristic features applicable to the general model of orthogneiss development? Most known orthogneisses are found in three types of structural setting: tangential structures, such as gneiss-cored nappes; domes; and crustal shears. In each setting a theoretical, typically non coaxial strain, operates at all stages of the formation of the structures. In general, this type of strain is difficult to demonstrate in view of the advanced stage of deformation attained in most of these structures.

In our opinion, the study presented here, and others in progress, indicate that non coaxial strain is one of the factors in almost every example of orthogneiss development. The process is fundamentally the sum of continuous and discontinuous deformation at the grain scale of a non deformed granular parent rock.

Acknowledgements—The authors are indebted to the members of the Laboratory of Structural Geology of the University of Rennes for their valuable discussion and critical comments. Special thanks are due to C. Audren, J. P. Brun, R. Capdevila, P. Cobbold, D. Gapais, S. K. Hanmer, J. L. Lagarde et C. Le Corre. This study forms part of the C.N.R.S. research programme "Déformation des roches", A.T.P. No. 1787.

REFERENCES

Arthaud, F. & Matte, P. 1975. Les décrochements tardi-hercyniens du sud-ouest de l'Europe. Géométrie et essai de reconstitution des conditions de la déformation. *Tectonophysics* **25**, 139–171.

Arthaud, F. & Matte, P. 1977. Late Paleozoic strike-slip faulting in southern Europe and northern Africa: result of a right-lateral shear zone between the Appalachians and the Urals. *Bull. geol. Soc. Am.* **88**, 1305–1320.

Bhattacharyya, D. S. & Pasayat, S. 1968. Deformation texture in quartz: a theoretical approach. *Tectonophysics* **5**, 303–314.

Bossiere, G. & Vauchez, A. 1978. Natural deformation by ductile shear in the west of Grande Kabilie (Algeria). *Tectonophysics* **51**, 57–81.

Boullier, A. M. & Guegen, Y. 1975. Origin of some mylonites by super-plastic flow. *Contrib. Mineral. Petrol.* **50**, 93–104.

Choukroune, P. & Lagarde, J. L. 1977. Plans de schistosité et déformation rotationnelle: l'exemple du gneiss de Champtoceaux (Massif Armoricain). *C.r. hebd. Séanc. Acad. Sci., Paris* **284**, 2331–2334.

Cogné, J. 1960. Schistes cristallins et granites en Bretagne méridionale: le Domaine de l'Anticlinal de Cornouaille (Thèse, Strasbourg). *Mém. Serv. Carte géol. det. Fr.* 1–382.

Cogné, J. 1966. Les grands cisaillements hercyniens dans le Massif Armoricain et les phénomènes de granitisation. In: *Etages Tectoniques*. Congrès Neufchatel, Ed. de la Bacconière, Neufchatel (Suisse), 179–192.

Cogné, J. 1977. La chaîne hercynienne ouest-européenne correspondelle à un orogène par collision? Proposition pour une interprétation géodynamique globale. *Coll. Int. CNRS,* **268**, 111–129.

Coward, M. P. 1976. Archean deformation patterns in Southern Africa. *Phil. Trans. R. Soc.* **A283**, 313–332.

Higgins, M. 1971. Cataclastic rocks. *Prof. Pap. U.S. geol. Surv.* **687**, 1–97.

Kroll, H. & Bambauer, H. V. 1971. The displacive transformation of (K, Na, Ca)-feldspars. *Neues Jb. Miner. Mh.* **9**, 413–416.

Lachenbruch, A. H. & Sass, J. H. 1973. Thermomechanical aspects of the San Andreas fault system. In: *Proceedings of a conference, Tectonic Problems of the San Andreas Fault System. Stanford Univ. Publs. Geol. Sci.* **13**, 192–209.

Laurent, P. & Burg, J. P. 1978. Strain analysis through a shear zone. *Tectonophysics* **47**, 15–42.

Means, W. D. 1977. A deformation experiment in transmitted light. *Earth Planet. Sci. Lett.* **35**, 169–179.

Ramsay, J. G. & Graham, R. H. 1970. Strain variation in shear belts. *Can. J. Earth Sci.* **7**, 786–813.

Roy, S. 1977. Mylonitic microstructures and their bearing on the development of mylonites — an example from deformed trondjhemites of the Bergen Arc region. SW Norway. *Geol. Mag.* **114**, 445–58.

Schmidt, S. M., Boland, J. N. & Paterson, M. S. 1977. Superplastic flow in finegrained limestone. *Tectonophysics* **43**, 257–292.

Tullis, J. & Yund, R. A. 1977. Experimental deformation of dry Westerly granite. *J. geophys. Res.* **83**, 5705–5718.

Vidal, Ph. 1973. Premières données géochronologiques sur les granites hercyniens du sud du Massif Armoricain. *Bull. Soc. géol. Fr.* 7 **Sér. t. 15**, 239–245.

White, S. 1976. The effects of strain on the microstructures, fabrics and deformation mechanisms in quartzites. *Phil. Trans. R. Soc.* **A283**, 69–86.